Electronic Supplementary Information for " An experimental study of indene pyrolysis with synchrotron vacuum ultraviolet photoionization mass spectrometry "

Hanfeng Jin[1], Jiuzhong Yang[2*], Lili Xing[3], Junyu Hao[1], Yan Zhang[2], ChuangChuang Cao[2], Yang Pan[2], Aamir Farooq[1*]

[1]*King Abdullah University of Science and Technology, [1]Clean Combustion Research Centre, Physical Sciences and Engineering Division, Thuwal 23955-6900, Saudi Arabia*

[2]*National Synchrotron Radiation Laboratory, University of Science and Technology of China, Hefei, Anhui 230029, China*

[3]*Vehicle & Transportation Engineering Institute, Henan University of Science and Technology, Luoyang, Henan 471003, China*

*Corresponding authors. E-mail: aamir.farooq@kaust.edu.sa (AF), jzhyang@ustc.edu.cn (JY), Tel: +966-128082704 (AF), +86-551-63602073 (JY).

1. Experimental details

1.1 Temperature profiles

Temperature of the flow reactor is controlled by W-Re thermocouple placed at the outside wall of the reactor. Thus, it is important to calibrate the temperature discrepancy between the control point and the reaction zone. Temperature profiles in the reaction zone are measured by an S-type thermocouple, as described in the previous study [1]. As shown in Fig. S1, values along the heating zone of the flow reactor are measured, where quartz nozzle is located at z = 0 mm. Temperature profiles are also used as the input parameters in the modeling work [2]. Temperature profiles at the specific reactor temperature can be calibrated from the interpolation of measured values.

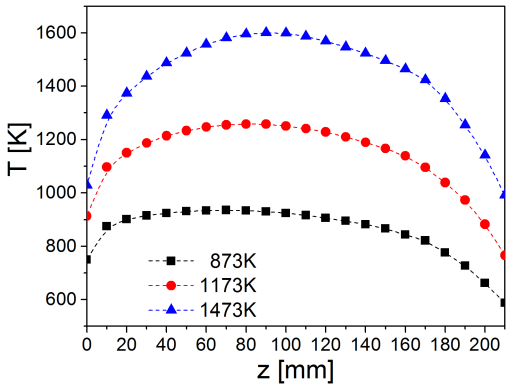

Figure S1 Temperature profiles measured along the flow reactor at three different reactor temperatures. Symbols indicates the values measured by an S-type thermocouple at the specific reactor temperature.

1.2 Purity of indene

The purity of indene used in this study is specified to be ≥97% (supplier: Alfa Aesar). The influence of fuel impurity on the study of kinetics should be analyzed before interpreting our experimental observations. Figure S2 presents the mass spectrum of indene sample by VUV soft photoionization. The highest mass peak is indene (m/z 116), and the small one (m/z 117) is its C^{13} isotopic peak. Very small peaks at m/z 118 and 134 are the impurities of indene sample, probably indane and t-butylbenzene. Their quantities are around 0.53% and 0.72% in the total (100%) sample. Such low level of impurity (~1.25%) is considered to be of negligible impact on the main conclusions of this experimental study.

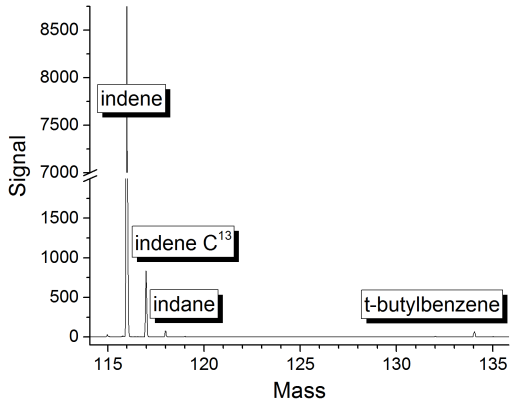

Figure S2 Mass spectrum of the impurities in fuel sample.

1.3 Carbon balance

Mass loss would be a considerable problem in the pyrolysis of indene, although we have performed our experiments in conditions with very low soot emissions. A check on the balance of mole fraction and carbon flux can help confirm the accuracy of our quantitative measurement. Total mole fraction is obtained by summing the contribution from all measured hydrocarbon species (X_{total} ideally equals to $1-X_{Ar} = 0.0032$), and carbon balance is expressed as the sum of carbon in all measured species divided by the inlet carbon flux of indene. Fig. S3 presents these balances over a range of temperatures at 30 and 760 torr. These results reveal very good conservation in the measurements. A carbon loss of less than 15% is very good for such a sooty reactant in pyrolytic process.

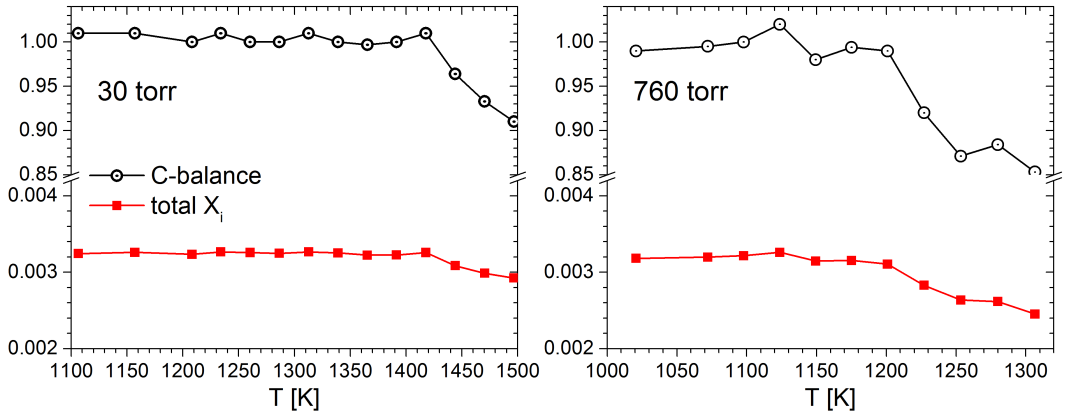

Figure S3 The balance of mole fraction and carbon flux in experiments at 30 and 760 Torr.

2. Photoionization cross-section (PICS)

2.1 Calibration of PICS

PICS of the reported species are referred to three sources: 1) direct calibration, like indene; 2) literature; 3) estimation *via* similar molecules. Nitric oxide (NO) is adopted as the reference species for the calibration of indene PICS. NO has many measurements in the literature, which provide reliable PICS. The data reported in the work of Watanabe et al. [3] is taken as a reference. Figure S4 presents perfect agreement between this measurement and the literature data, and verifies the accuracy of PICS measurement by this method. The PICS of indene can be calculated by the expression below (Eq. S1), in which S is the mass signal, X is the mole fraction, σ is the cross-section, and D is the mass discrimination factor [4]. The PICS of indene and 3-methyl-indene are presented in Figs. S5 and S6. The measurement shows that fragmentation of indene occurs when the photon energy is higher than 12.3 eV, producing a $C_9H_7^+$ ion.

$$\sigma_{indene} = \sigma_{NO} \times \frac{S_{indene}}{S_{NO}} \times \frac{X_{NO} D_{NO}}{X_{indene} D_{indene}} \qquad \text{Eq. S1}$$

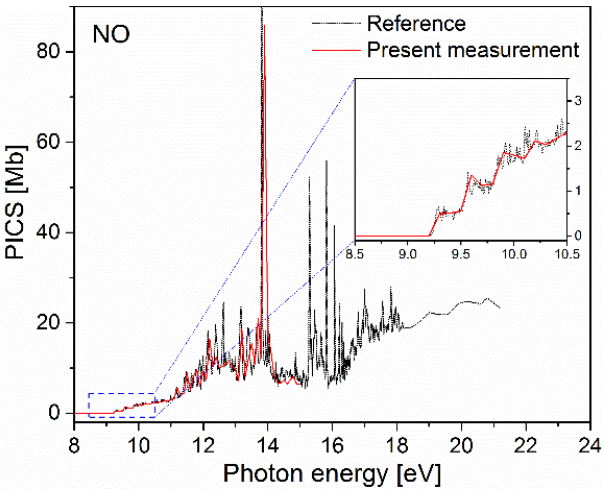

Figure S4 PICS of NO; comparison between this work and reference data [3].

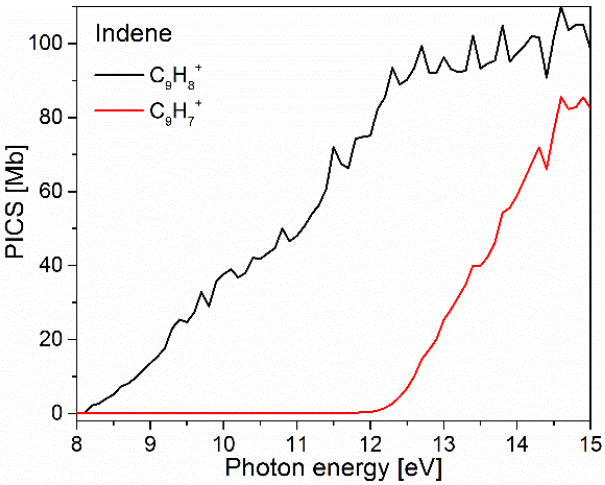

Figure S5 PICS of indene. The black line indicates the cross section of $C_9H_8^+$ ion, and red line indicates that of $C_9H_7^+$ ion, which is a fragment of $C_9H_8^+$.

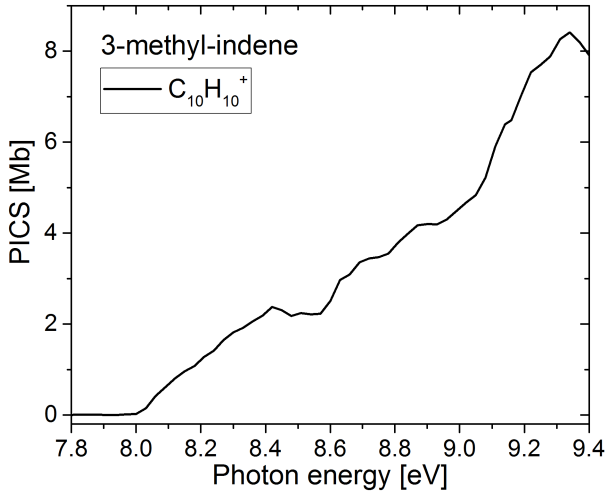

Figure S6 PICS of 3-methyl-indene.

2.2 References of PICS

Table S1 below provides the PICS references adopted in the calculation of the species reported in this work. The mass, name, structure and abbreviation of these species are provided, as well as the reference literature of their cross-sections.

Table S1 PICS references of reported species

Mass	Abbreviation	Name[c]	Reference
26	C_2H_2	acetylene	Cool et al.[a,5]
39	C_3H_3	propargyl	Savee et al.[a,6]
40	aC_3H_4	allene	Yang et al.[a,7]
40	aC_3H_4	propyne	Cool et al.[a,5]
50	C_4H_2	butadiyne	Cool et al.[a,5]
52	C_4H_4	vinyl-acetylene	Cool et al.[a,5]
65	C_5H_5	cyclopentadienyl	Hansen et al.[a,8]
66	C_5H_6	cyclopentadiene	Hansen et al.[a,8]
78	C_6H_6	benzene	Cool et al.[a,5]
92	C_7H_8	toluene	Zhou et al.[a,9]
102	C_8H_6	phenylacetylene	Zhou et al.[a,9]
116	C_9H_8	indene	pw.[b]
130	$C_9H_7CH_3$	3-methyl-indene	pw.[b]
202	$C_{16}H_{10}$	pyrene	Johansson et al.[10]
228	$C_{18}H_{12}$	chrysene	Johansson et al.[10]

a. Refer to Photoionization Cross Section Database (Version 2.0)[11] for the estimated PICS.
b. Measured in this work.
c. Calibrated as this structure in mole fraction calculation.

References

1 Z. Zhou, X. Du, J. Yang, Y. Wang, C. Li, S. Wei, L. Du, Y. Li, F. Qi and Q. Wang, *J. Synchrot. Radiat.*, 2016, **23**, 1035-1045.

2 Y. Zhang, J. Cai, L. Zhao, J. Yang, H. Jin, Z. Cheng, Y. Li, L. Zhang and F. Qi, *Combust. Flame*, 2012, **159**, 905-917.

3 K. Watanabe, Matsunag.Fm and H. Sakai, *Appl. Opt.*, 1967, **6**, 391-396.

4 T. A. Cool, K. Nakajima, C. A. Taatjes, A. McIlroy, P. R. Westmoreland, M. E. Law and A. Morel, *Proc. Combust. Inst.*, 2005, **30**, 1681-1688.

5 T. A. Cool, J. Wang, K. Nakajima, C. A. Taatjes and A. McIlroy, *Int. J. Mass Spectrom.*, 2005, **247**, 18-27.

6 J. D. Savee, S. Soorkia, O. Welz, T. M. Selby, C. A. Taatjes and D. L. Osborn, *J. Chem. Phys.*, 2012, **136**, 134307.

7 B. Yang, J. Wang, T. A. Cool, N. Hansen, S. Skeen and D. L. Osborn, *Int. J. Mass Spectrom.*, 2012, **309**, 118-128.

8 N. Hansen, S. J. Klippenstein, J. A. Miller, J. Wang, T. A. Cool, M. E. Law, P. R. Westmoreland, T. Kasper and K. Kohse-Höinghaus, *J. Phys. Chem. A*, 2006, **110**, 4376-4388.

9 Z. Y. Zhou, M. F. Xie, Z. D. Wang and F. Qi, *Rapid Commun. Mass Spectrom.*, 2009, **23**, 3994-4002.

10 K. O. Johansson, M. F. Campbell, P. Elvati, P. E. Schrader, J. Zádor, N. K. Richards-Henderson, K. R. Wilson, A. Violi and H. A. Michelsen, *J. Phys. Chem. A*, 2017, **121**, 4447-4454.

11 Photonionization Cross Section Database (Version 2.0), http://flame.nsrl.ustc.edu.cn/en/database.htm, National Synchrotron Radiation Laboratory, Hefei, China, 2017.